PB87-145991

Three-Dimensional Model for Hyperthermia Calculations

(U.S.) Health Effects Research Lab.
Research Triangle Park, NC

Jan 87

U.S. Department of Commerce
National Technical Information Service
NTIS

PB87-145991

EPA/600/D-87/015
January 1987

A THREE-DIMENSIONAL MODEL FOR HYPERTHERMIA CALCULATIONS

by

R. J. Spiegel[1] and M. B. E. Fatmi[2]

[1]Health Effects Research Laboratory, U.S. Environmental Protection Agency, Research Triangle Park, NC 27711

[2]Northrop Services, Inc., Research Triangle Park, NC 27709

HEALTH EFFECTS RESEARCH LABORATORY
OFFICE OF RESEARCH AND DEVELOPMENT
U.S. ENVIRONMENTAL PROTECTION AGENCY
RESEARCH TRIANGLE PARK, NC 27711

REPRODUCED BY
U.S. DEPARTMENT OF COMMERCE
NATIONAL TECHNICAL
INFORMATION SERVICE
SPRINGFIELD, VA. 22161

TECHNICAL REPORT DATA *(Please read Instructions on the reverse before completing)*		
1. REPORT NO. EPA/600/D-87/015	2.	3. RECIPIENT'S ACCESSION NO. PB87 145991/AS
4. TITLE AND SUBTITLE A Three-Dimensional Model for Hyperthermia Calculations		5. REPORT DATE January 1987 6. PERFORMING ORGANIZATION CODE
7. AUTHOR(S) R.J. Spiegel, HERL, EBD, BEB* M.B.E. Fatmi, NSI, Inc. +		8. PERFORMING ORGANIZATION REPORT NO.
9. PERFORMING ORGANIZATION NAME AND ADDRESS U.S. Environmental Protection Agency * Northrop Services, Inc. +		10. PROGRAM ELEMENT NO. 11. CONTRACT/GRANT NO.
12. SPONSORING AGENCY NAME AND ADDRESS Health Effects Research Laboratory, RTP Office of Research and Development U.S. Environmental Protection Agency Research Triangle Park, NC 27711		13. TYPE OF REPORT AND PERIOD COVERED 14. SPONSORING AGENCY CODE EPA/600/11
15. SUPPLEMENTARY NOTES		

16. ABSTRACT

Realistic three-dimensional models that predict temperature distributions with a high degree of spatial resolution in bodies exposed to electromagnetic (EM) fields are required in the application of hyperthermia for cancer treatment. To ascertain the thermophysiologic response of humans during hyperthermia, a finite-difference procedure for calculating both the EM deposition and heat transfer within the body has been developed. This model possess sufficient spatial resolution to consider basic anatomical features including organs and tumors. The flow of heat into and out of the body has been simulated; this includes internal heat generation (metabolism and EM deposition), cooling and distribution of heat by blood flow, thermal conduction throughout the body, evaporative heat loss, and radiation and convection from the outer surface of the body to the environment. Dynamic thermoregulatory behavior such as peripheral vasomotor responses (skin vasodilation and vasoconstriction) and variable sweating rates were also simulated. Two hyperthermia scenarios were studied with the model.

17. KEY WORDS AND DOCUMENT ANALYSIS		
a. DESCRIPTORS	b. IDENTIFIERS/OPEN ENDED TERMS	c. COSATI Field/Group
18. DISTRIBUTION STATEMENT RELEASE TO PUBLIC	19. SECURITY CLASS *(This Report)* UNCLASSIFIED 20. SECURITY CLASS *(This page)* UNCLASSIFIED	21. NO. OF PAGES 10 22. PRICE

EPA Form 2220-1 (Rev. 4-77) PREVIOUS EDITION IS OBSOLETE

NOTICE

This document has been reviewed in accordance with U.S. Environmental Protection Agency policy and approved for publication. Mention of trade names or commercial products does not constitute endorsement or recommendation for use.

A Three-Dimensional Model for Hyperthermia Calculations

R.J. Spiegel[1] and M.B.E. Fatmi[2]

[1]U.S. Environmental Protection Agency
Research Triangle Park, NC 27711
[2]Northrop Services, Inc.
Research Triangle Park, NC 27709

ABSTRACT

Realistic three-dimensional models that predict temperature distributions with a high degree of spatial resolution in bodies exposed to electromagnetic (EM) fields are required in the application of hyperthermia for cancer treatment. To ascertain the thermophysiologic response of humans during hyperthermia, a finite-difference procedure for calculating both the EM deposition and heat transfer within the body has been developed. This model possess sufficient spatial resolution to consider basic anatomical features including organs and tumors. The flow of heat into and out of the body has been simulated; this includes internal heat generation (metabolism and EM deposition), cooling and distribution of heat by blood flow, thermal conduction throughout the body, evaporative heat loss, and radiation and convection from the outer surface of the body to the environment. Dynamic thermoregulatory behavior such as peripheral vasomotor responses (skin vasodilation and vasoconstriction) and variable sweating rates were also simulated. Two hyperthermia scenarios were studied with the model.

INTRODUCTION

One of the most important challenges in clinical hyperthermia is the acquision of temperature information throughout the treatment volume (tumor and surrounding normal tissue). However, in practice temperature information can be measured only at a few selected locations. What is required is an accurate computer model to predict the temperature profile and thermoregulatory response of the patient during exposure to electromagnetic (EM) fields produced by an applicator. Thus, a combined EM deposition and thermoregulatory model must be developed for this task. The EM deposition model must provide an accurate determination of the specific absorption rate (SAR), which is the mass-normalized rate of energy absorbed as specified in terms of W/kg or W/g, throughout an anatomically realistic exposure volume. In this regard, it is important to realize that the exposure volume and treatment volume may not be identical because, as pointed out recently (1), a significant amount of EM energy can be deposited outside the intended treatment area. The thermoregulatory system model must simulate the flow of heat into and out of the body, including internal heat generation (metabolism) of the body and the heat produced by the EM field, cooling and distribution of heat by blood, evaporative heat loss from sweating, and radiation and convection from the outer surface of the body. In addition, the thermoregulatory system should attempt to simulate dynamic thermoregulatory actions such as cutaneous vasodilation, variable internal blood flow rates, and variable sweating rates.

Two-dimensional hyperthermia related simulations (2) have been utilized for this task. While these models have provided useful information relative to cross sectional temperature profiles during exposure, it can be expected that the predictions of these models are, at best, gross estimates of the actual values. For example, so-called aberrant heating (energy deposition outside the treatment region) cannot be treated by two-dimensional simulations. A more fundamental limitation of two-dimensional models is that they cannot provide an adequate representation of the human thermoregulatory system.

This paper describes a more realistic three-dimensional model to ascertain the thermophysiologic response of humans during hyperthermia. The model is based on a finite difference (FD) numerical technique which divides the body into a large number of small blocks or cells. Models with over 100,000 cells are possible, but the model presented here is comprised of a few thousand cells. The thermal model considers active mechanisms of thermoregulation such as vasodilation and sweating, as well as the passive modes of heat transfer (conduction, convection, and radiation). The method is general and can predict SARs and temperatures in complex spatial geometries in which metabolic rates and blood flow rates can vary with tissue type and with time. The model is illustrated by the determination of the heating patterns produced by EM energy deposited in the torso and in the thigh.

THERMOREGULATORY MODEL

Figure 1 illustrates, in block diagram form, the

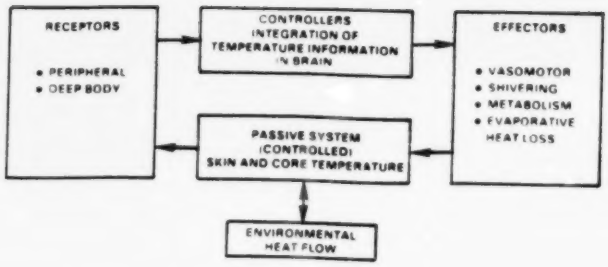

Figure 1. Block diagram of the basic thermoregulatory system (3).

basic components needed to study human thermoregulation. The thermoregulatory system consists of two major parts: an active or controlling system and a passive or controlled system. The controlling system consists of a hypothalamic controller in the brain and associated afferent and efferent pathways. This controller receives afferent signals from thermoreceptors in the skin and body core, integrates this temperature information, compares the results with set point temperatures, and produces the appropriate alteration in vasomotor response, sweating, or shivering via efferent pathways. Note, that these thermoreceptors are either "warm" or "cold" receptors. Upon sudden warming, a "warm" receptor will produce electrical impulse signals that are carried by neural pathways to appropriate locations. A decrease in the production of signals occurs when the area is suddenly cooled. A "cold" receptor acts in the opposite fashion; it increases the production of signals when a drop in the local temperature occurs. The controlled heat transfer system represents the passive modes of heat transfer (conduction, convection, and radiation) within and from the surface of the body.

The engineering or physical model for the human thermoregulatory system consists of two major parts: a controlled system and a controlling system. The controlled system is modeled by a transient heat conduction model, with the controlling system providing physiologically relevant thermal boundary conditions to maintain homeothermy. The controlling system incorporates set point or reference temperatures as the preferred body temperatures. The mathematical simulation attempts to maintain those set point temperatures by calculating the deviation between the set point temperatures and the actual body temperatures. This deviation represents an error signal; the magnitude of the response is directly related to the size of the error signal.

Controlled System

The controlled system is a transient heat conduction model which includes internal heat generation and heat dissipation. The internal heat generation results from body metabolism. The internal heat dissipation occurs by convective exchange with the cardiovascular system and a combined convective and radiant exchange with the surrounding environment at the surface of the skin and respiratory tract.

To solve the heat transfer equation, a model was constructed from 1172 rectangular blocks. The model utilizes rectangular blocks to configure the geometry primarily because the future use of this model will be in conjunction with an EM deposition model. Heat transfer analyses allow for more realistic block treatment, but currently available EM deposition models do not (4).

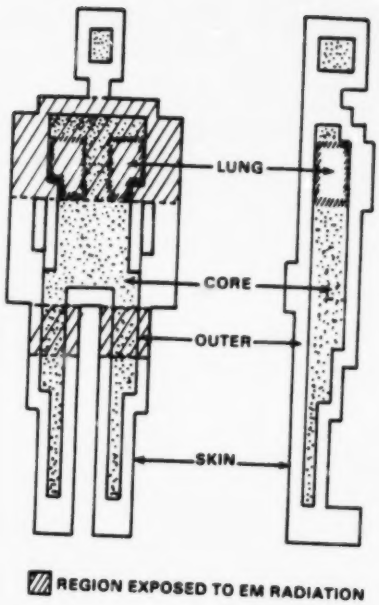

Figure 2. Front and side views of the block model of a human in cross section taken through the mid-frontal and mid-sagittal planes of the body and the midlines of the arms and legs.

The model represents a spatial approximation of a human in an upright position with a height of 180 cm and a weight of 105 kg. Because of difficulties in approximating the curved portions of the body with rectangular blocks, the surface area in relation to body weight is 18% larger in this model than the average value as calculated by the Dubois formula (5).

Figure 2 illustrates the block model. Note that it contains four distinct types of material: a core, lung tissue, an outer layer, and skin. The core of the torso and head is comprised of viscera, skeleton, and connective tissue, whereas the core of the legs is composed of skeleton and connective tissue. The outer layer is a composite layer of muscle and fat. The tissue distribution and the fractional volume for the core and outer layers are based on information described by Stolwijk (6) for his human model. Because the thickness of the skin layer is very small, it was assumed to have zero thickness for modeling purposes. How these volumes with no mass are handled in the heat transfer calculations is described below.

The finite-difference solution is achieved by representing the mass of each rectangular block of Figure 2 by a node which is placed in the center of the block. The paths for heat flow between the nodes are represented by heat conductors that are connected to the nodes. The thermal energy of each node is represented by a capacitor whose value is the amount of heat required to raise the temperature of the mass 1 C. Thus, the problem is reduced to a thermal network where the temperature at each node is determined by solving the following finite difference equation (7):

$$(C_i/\Delta t)(T_i^{m+1}-T_i^m) = \sum_j K_{ij}(T_j-T_i)^m + Q_i \qquad (1)$$

where $C_i = \rho c \Delta V$ = thermal capacitance of node i,

ρ = density of tissue,

ΔV = volume of block associated with node i,
c = specific heat of tissue,
Δt = time interval,
K_{ij} = conductor for conduction, convection, or radiation,
K_{ij} = kA/Δd = conductor value for conduction,

A = cross-sectional area perpendicular to the direction of heat transfer,
k = thermal conductivity of tissue,
Δd = distance between nodes of the conductor,
K_{ij} = hA = conductor value for convection,

h = convective heat transfer coefficient,
K_{ij} = conductor for radiation

$$= \sigma AF(T_j^2+T_i^2)^m(T_j+T_i)^m$$

σ = Stefan-Boltzman constant,
F = geometrical "view" factor,
Q_i = heat sources (metabolic, evaporation, and EM)

T_i^m = present temperature of node i,

T_i^{m+1} = future temperature of node i, and

T_j^m = present temperature of node j.

From knowledge of the surface area, the volume, and the tissue composition of each block, values can be determined for the conductors associated with conduction, convection, and radiation. Further, when Equation (1) is rearranged so that all the terms involving the present temperatures (level m) are on the same side of the equation, then

$$T_i^{m+1} = T_i^m + (\Delta t/C_i)S \qquad (2)$$

where S is a composite term that contains all those individual terms on the right hand side of Equation (1). Thus, Equation (2) is an explicit expression that calculates new temperatures from old temperatures. The successive application of the formula at each node yields the new temperatures at every node in the network. This can be repeated until steady-state conditions are reached. To insure stability of the solution, the time interval Δt must be chosen so that it is less than or equal to the most restrictive value as based on the nodal relation that contains the smallest capacitance and the largest total conductance.

Nodes that represent the skin layer are given special treatment. Namely, because the layer is thin and knowledge of the temperatures inside the layer is not needed, its volume or mass is neglected. On the other hand, calculation of temperatures at the surface is important because heat transfer modes such as convection, radiation, and evaporation are directly dependent on surface temperatures. These nodes are, therefore, designated as interface nodes having zero thermal capacitance. Nodal temperatures are calculated by Equation (1) with $C_i = 0$, that is,

$$T_{i+1}^m = (\sum_j K_{ij}\, T_i^m + Q_i)/\sum K_{ij} \qquad (3)$$

In other words, the nodal temperatures are determined by assuming the heat that enters each node also leaves it, and consequently the presence of these nodes does not affect the temperatures of those nodes on either side of the interface.

The model also utilizes one node for the central blood pool and one for the external environment.

The thermal network which approximates the controlled system consists of a total 2359 nodes connected together by 8752 thermal conductors, 2359 thermal capacitors, and 5902 thermal sources (1186 evaporative, 2358 metabolic and 2358 EM). The transient temperature profile can be calculated for each node, that is, at 2359 interior and surface locations.

Blood flow rates. Conductor values for convective heat exchange between each node and the central blood pool depend on the blood flow rates. Because blood flow plays a major role in heat transfer within the body, these terms will be explained further. A marked redistribution of blood flow occurs when humans are heat stressed. In general, the skin blood flow is sharply increased (vasodilation) whereas blood flow to visceral organs and muscle tissue declines or is at basal levels. When the ambient temperature is below the thermoneutral zone, skin blood flow is reduced (vasoconstriction). Thus, the skin blood flow is highly dependent upon ambient temperature, as well as the EM heat load. Active vasodilation, along with increased sweating, represents the body's major adjustment to heat loads.

Utilizing the same approach as that by Stolwijk (6) in his human model, an empirical relation for local skin blood flow is given by the expression

$$BF_i = \frac{[BFB_i + \alpha_i \cdot DILAT]2^{(T_i-T_{i,set})/10}}{1 + \beta_i \cdot STRIC} \qquad (4)$$

where
BFB_i = local basal blood flow rate,

T_i = local skin temperature,

$T_{i,set}$ = local skin set point temperature,

DILAT = total controller command for skin vasodilation,
STRIC = total controller command for skin vasoconstriction,
α_i = fraction of DILAT command applicable to skin of node i, and
β_i = fraction of STRIC command applicable to skin of node i.

In the equation, the terms DILAT and STRIC are controller equations which will be discussed later (see section on controlling system). The weighted vasodilation command $\alpha_i \cdot$DILAT is added to the basal blood flow to increase skin blood flow in response to increased body temperatures. The weighted vasoconstriction command $\beta_i \cdot$STRIC acts to reduce blood flow in response to decreased body temperatures. As will be shown later, the DILAT and STRIC commands are functions of both the integrated skin response and the difference between brain temperature and its set point temperature; however, it is also known that local skin temperature affects blood flow. Therefore, the exponential term in the expression accounts for the local temperature effect. It doubles the blood flow rate for every 10 C increase in local temperature above the set point temperature and cuts the flow in half for a 10 C drop in temperature. Note also that the controller commands DILAT and STRIC do not act simultaneously. If vasodilation occurs, then STRIC = 0; when vasoconstriction takes place, DILAT = 0.

During conventional environmental exposure (no EM heat load) blood flow in muscle tissue is essentially controlled by the metabolic demand for oxygen. Muscle blood flow is increased when oxygen requirements increase as a result of work activity or shivering. Shivering is initiated when the body is subjected to a sufficiently low ambient temperature (<28 C for a nude

subject). It is also known that muscle tissue increases blood flow in response to large SARs in the tissue as a result of EM exposure. This increase occurs when the tissue temperature reaches approximately 40 C. Therefore, in this study muscle blood flow is fixed at basal levels (the subject is situated in an ambient air temperature >28 C and is in a sedentary state) until the tissue temperature exceeds 40 C and then the flow is allowed to increase at a rate of 33% of the basal level per C and is capped off at twice the basal level at 46 C.

The model sets all core blood flow rates at the basal values.

Heat sources and sinks. The other heat exchange modes contained in Equation (1) are the heat sources and sinks (Q_i). These include metabolic heat production, heat loss by sweat evaporation from the skin, and EM induced heat.

The body has its own source of heat production by metabolic activity. In muscle tissue, the metabolic rate can be accelerated above basal levels as a result of work activity and shivering. The total basal metabolic heat production is 105 W. The distribution in the various regions (torso, arms, legs, etc.) is proportioned according to that specified by Stolwijk (6). The metabolic heat sources for the individual nodes in the thermal network are determined by distributing to total metabolic rate for that region in proportion to the respective weight of the block that a node represents.

Heat lost due to sweating is a major avenue by which the body regulates internal temperatures. Several mathematical models have been proposed to calculate heat loss by sweating. They are all empirical and attempt to give a best-fit to experimental data for various conditions. The equation used by Stolwijk (6) takes the form

$$Q_{E,i} = (QB_{E,i} + S_i \cdot SWEAT)2^{(T_i - T_{i,set})/10} \qquad (5)$$

where

$QB_{E,i}$ = basal evaporative heat loss,

SWEAT = total controller command for sweating,

S_i = fraction of sweating command applicable to skin of segment i,

T_i = local skin temperature, and

$T_{i,set}$ = local skin temperature.

Note that general form of this expression is very similar to Equation (4). For a given value of the controller command SWEAT, it is evident that the skin sweats more at a higher local skin temperature than a lower temperature. As will be explained later, SWEAT is a function of hypothalamic and mean skin temperatures; thus, the local sweating response is both an additive and multiplicative function of the local skin, core, and mean skin temperatures. The quantity S_i accounts for the fact that sweat production is not uniformly distributed over the surface of the body. There is a maximum rate of evaporation that is possible for a given set of environmental conditions. This maximum value depends on water vapor pressure at the surface of the skin. If $Q_{E,i}$ exceeds the maximum value, then it is set equal to the allowed maximal limit.

The thermal loading due to energy absorbed from an EM field is accounted for by an additional heat source for each node. The mass-normalized rate of energy absorption or SAR at a specific location is given by the expression

$$SAR = \frac{\sigma |E|^2}{\rho} \qquad (6)$$

where E is the RMS value of the internal field strength, σ is the tissue conductivity, and ρ is the tissue mass density. Thus, the localized SAR is directly related to the internal electric field and the numerical procedures all involve the determination of the electric field distribution within the biological body. The finite-difference approach has been described elsewhere (8). After the SAR has been determined, the heat source for each node is determined by multiplying the SAR by the weight of the block that each node represents. As a result, a distribution of EM induced heat sources is specified for the thermal network.

Controlling System

Physical or engineering models of the controller system incorporate set point or reference temperatures and a deviation between the set point temperature and the actual temperature represents an error signal. The magnitude of the response is directly related to the size of the error signal and thermal response (vasoconstriction, vasodilation, and sweating) can be approximated by a general controller expression

$$CONTROL = A(T_H - T_{H,set}) + B\sum D_i(T_i - T_{i,set}) \qquad (7)$$

The term $(T_H - T_{H,set})$ represents the difference between brain termperature and its set point temperature. It accounts for the thermoreceptors in the hypothalamus. The second quantity in the expression represents the total integrated difference between the skin temperatures and the skin set point temperature, where the summation is across all skin nodes. Thus, the error signal is determined according to the values for $(T_H - T_{H,set})$ and $(T_i - T_{i,set})$: positive values are warm receptor outputs and negative values imply cold receptor outputs. This controller equation is used to affect the vasomotor response through the DILAT and STRIC commands in Equation (4) and the sweating response via the SWEAT command in Equation (5). If the error signal is positive, then the DILAT and SWEAT commands are activated. A negative error signal implies that STRIC is activated; however, the value that is substituted into Equation (4) is the magnitude of the error signal. The quantities A and B are empirical constants and are designated as control coefficients. Values for these quantities have been specified elsewhere (6). Values for D, the fraction of the skin receptors associated with each node, are determined by assuming a uniform distribution over the body. Thus, the value of D for node i would be determined by dividing the surface area associated with node i by the total surface area of the body.

NUMERICAL RESULTS

To demonstrate the model's ability to calculate the thermoregulatory profile for various hyperthermia scenarios, numerical results will be presented for EM energy being deposited in two treatment regions: the upper torso and the thigh. Only idealized applicators are considered; that is, it is assumed that the SAR is deposited uniformly throughout the treatment region. As mentioned earlier, the computer model can calculate SAR distributions for generalized exposure conditions (8), however, the purpose here is to highlight the thermal model and its capabilities.

The thermal model is executed for an ambient air

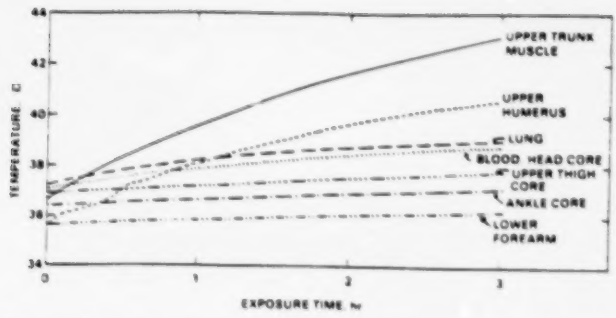

Figure 3. Selected internal temperatures versus exposure time when the EM energy is deposited in the upper torso and arms.

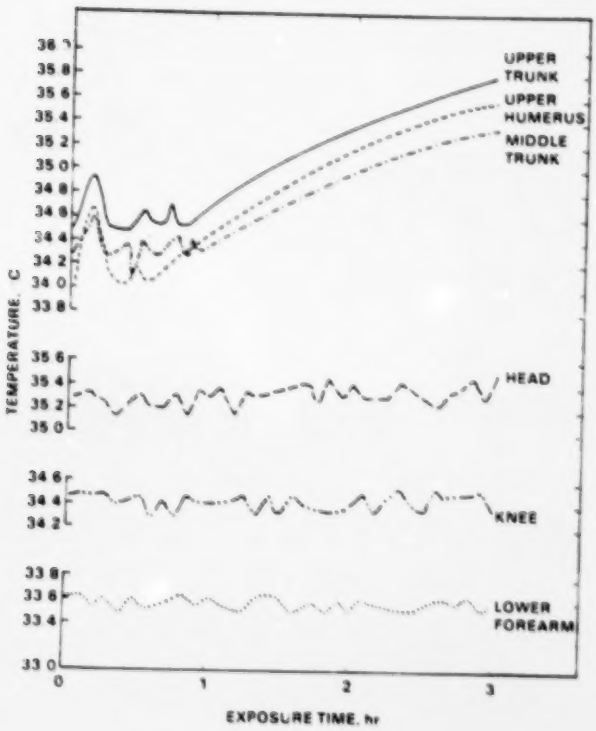

Figure 4. Selected skin temperatures versus exposure time when the EM energy is deposited in the upper torso and arms.

temperature of 30 C, a relative humidity of 50%, and still air (wind velocity 0.1 m/s). The program is executed for three hours exposure time or until thermal steady state conditions are reached, as specified by a temperature difference for consecutive iterations of 0.0001 C for all the nodes. The iteration time step between calculations is 30 s, as based on the smallest block in the model.

The set point temperatures are used as the initial temperature values for all the nodes. These set point temperatures, Tset, contained in Equations (4), (5) and (7) represent the temperatures the thermoregulation system attempts to maintain. For a nude, resting man, a thermal neutral environment implies an ambient temperature of 30 C and 30% relative humidity. Set point temperatures are determined for these conditions by solving Equation (1) with the blood flow set at basal levels and no sweating; that is, the controlling system (DILAT, STRIC, and SWEAT) is not activated. The resultant steady-state temperatures for all the nodes are the set point temperatures.

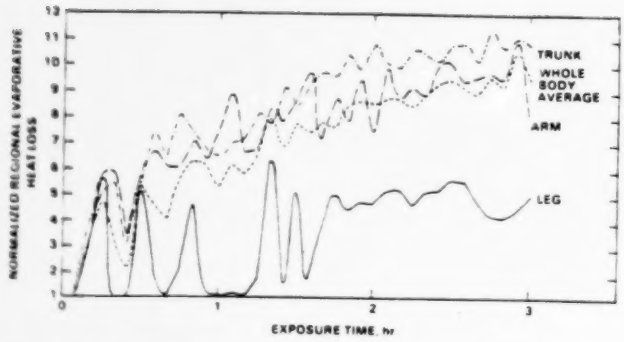

Figure 5. Normalized evaporative heat loss versus exposure time when the EM energy is deposited in the upper torso and arms.

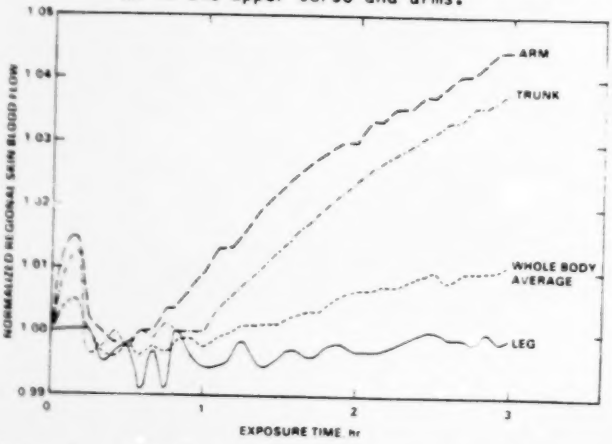

Figure 6. Normalized skin blood flow versus exposure time when the EM energy is deposited in the upper torso and arms.

Figures 3 through 6 contain selected calculated results versus exposure time when approximately 141 W is deposited uniformly throughout the upper torso and arms (see Figure 2). This EM deposition is approximately 1.3 times larger than the body's metabolic rate and corresponds to a treatment region SAR of 4 W/kg. Figures 3 and 4 contain plots of selected internal and skin temperatures, respectively. As would be expected, the significant temperature increases (both internal and skin) occur in the treatment volume. Very minimal temperature changes occur elsewhere. Figures 5 and 6 show the results for normalized regional evaporative heat loss and skin blood flow, respectively. It is especially noteworthy to observe in Figure 5 that the whole body evaporative heat loss increases measurably above basal levels during the course of the exposure. In addition, the leg exhibits a relatively large increase in sweating, even though no EM energy was deposited there. Skin vasodilation, however, was essentially restricted to the treatment region (see Figure 6).

Figures 7 through 10 summarizes the thermoregulatory response when 46 W of EM energy is deposited in the thigh (see Figure 2). Note that the treatment region

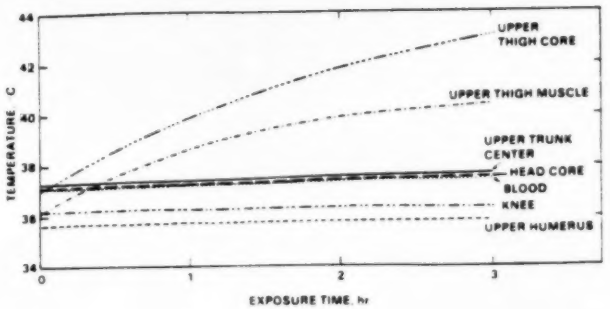

Figure 7. Selected internal temperatures versus exposure time when the EM energy is deposited in the upper thigh.

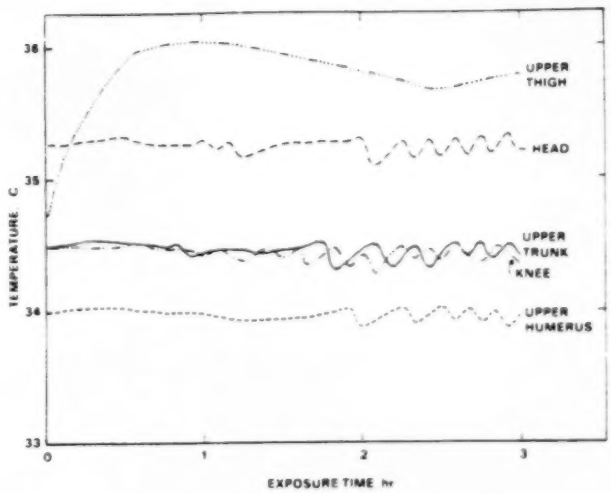

Figure 8. Selected skin temperatures versus exposure time when the EM energy is deposited in the upper thigh.

SAR is the same as the prior case, that is, 4 W/kg. As shown in Figure 7 and 8 only the thigh region exhibits temperature increases over initial values. Observe that the thigh skin temperature raises quickly, and then decreases. This thigh skin temperature decrease is produced by a significant increase in the thigh sweating rate (see Figure 9) during the exposure period. The minor transient variation in the other skin temperatures (head, trunk, knee, and arm) is caused by sweating rate changes at the site. As contained in Figure 10 thigh vasodilation rapidly occurs, but the concommitant thigh sweating rate increase produces significant heat loss from this region which, in turn, causes the vasodilation to diminish.

DISCUSSION

The main objective of this paper was to describe a realistic three-dimensional thermoregulatory model which can be used for hyperthermia calculations. Finite-difference procedures are utilized, and both the EM deposition and heat transfer within the body can be ascertained. For illustrative purposes, a human model comprised of 1172 blocks was used to calculate the thermoregulatory profiles for two different treatment regions.

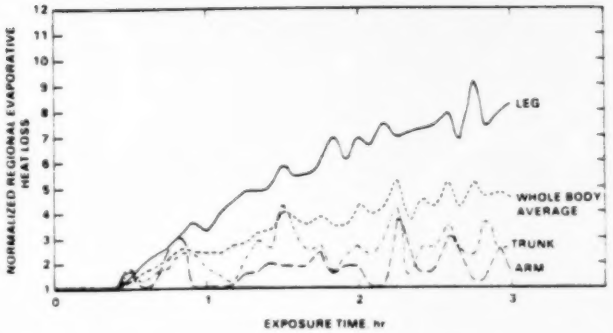

Figure 9. Normalized evaporative heat loss versus exposure time when the EM energy is deposited in the upper thigh.

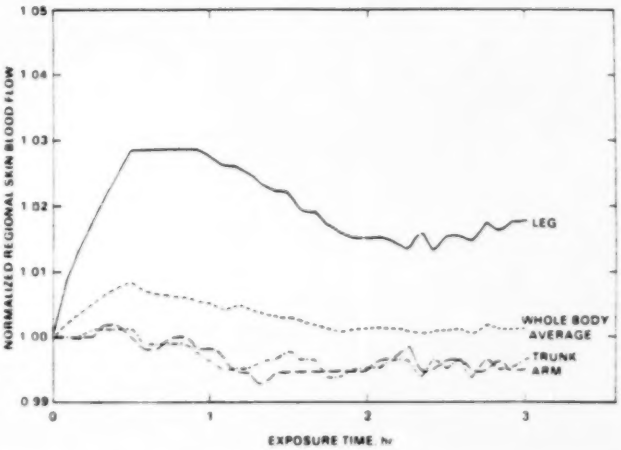

Figure 10. Normalized skin blood flow versus exposure time when the EM energy is deposited in the upper thigh.

When the model is executed on mainframe computers with at least 20 or 30 M bytes of fast (electronic) memory, models with at least 100,000 cells are possible. This would imply that the spatial resolution which can be obtained is on the order of 1 X 1 X 1 cm for a uniform distribution of cells. However, much finer resolution can be gained at one location at the expense of less resolution at others. Thus, the capability exists to model both the tumor and immediate surrounding normal tissue with a high degree of resolution, and also include the rest of the body in the simulation.

REFERENCES

1. Hagmann, M.J. and Levin, R.L., "Aberrant Heating: A Problem in Regional Hyperthermia," IEEE Trans. on Biomedical Engineering, Vol. BME-33, No. 4, pp. 405-411, 1986.
2. Strohbehn, J.W. and Roemer, R.B., "A Survey of Computer Simultations of Hyperthermia Treatments," IEEE Trans. on Biomedical Engineering, Vol. BME-31, No. 1, pp. 136-149, 1984.
3. Gordon, C.J., "A Review of Terms for Regulated vs. Forced Neurochemical-Induced Changes in Body Temperatures," Life Sci., Vol. 32, pp. 1285-1295, 1983.

4. Spiegel, R.J., "A Review of Numerical Models for Predicting the Energy Deposition and Resultant Thermal Response of Humans Exposed to Electromagnetic Fields," IEEE Trans. Microwave Theory and Techniques, Vol. MTT-32, No. 8, pp. 730-746, 1984.
5. Dubois, D. and Dubois, E.F., "A Formula to Estimate the Approximate Surface Area if Height and Weight be Known," Arch. Internal Medicine, Vol. 17, pp. 863-871, 1915.
6. Stolwijk, J.A.J., "A Mathematical Model of Physiological Temperature Regulation in Man," NASA CR-1855 (NTIS N 71-33401), Washington, DC, 1971.
7. Holman, J.P., Heat Transfer, 4th Edition , McGraw-Hill, NY, pp. 131, 1981.
8. Spiegel, R.J., Fatmi, M.B.E., and Kunz, R.S., "Application of a Finite-Difference Technique to the Human Radiofrequency Dosimetry Problem," J. of Microwave Power, pp. 241-253, 1985.

DISCLAIMER

The research described in this article has been reviewed by the Health Effects Research Laboratory, US Environmental Protection Agency and approved for publication. Approval does not signify that the contents necessarily reflect the views and policies of the Agency nor does mention of trade name or commercial products constitute endorsement or recommendation for use.